

Novel Pressure Phase Diagram of Heavy Fermion Superconductor CePt₃Si Investigated by ac Calorimetry*

Naoyuki TATEIWA^{1†}, Yoshinori HAGA¹, Tatsuma D. MATSUDA¹, Shugo IKEDA^{1,2},
Takashi YASUDA², Tetsuya TAKEUCHI³, Rikio SETTAI² and Yoshichika ÔNUKI^{1,2}

¹Advanced Science Research Center, Japan Atomic Energy Research Institute, Tokai, Ibaraki 319-1195

²Department of Physics, Graduate School of Science, Osaka University, Toyonaka, Osaka 560-0043

³Low Temperature Center, Osaka University, Toyonaka, Osaka 560-0043

The pressure dependences of the antiferromagnetic and superconducting transition temperatures have been investigated by ac heat capacity measurement under high pressures for the heavy-fermion superconductor CePt₃Si without inversion symmetry in the tetragonal structure. The Néel temperature $T_N = 2.2$ K decreases with increasing pressure and becomes zero at the critical pressure $P_{AF} \simeq 0.6$ GPa. On the other hand, the superconducting phase exists in a wider pressure region from ambient pressure to about 1.5 GPa. The pressure phase diagram of CePt₃Si is thus very unique and has never been reported before for other heavy fermion superconductors.

KEYWORDS: heavy-fermion superconductor, CePt₃Si, ac calorimetry

Recently, Bauer *et al.* reported superconductivity in CePt₃Si with a non-centrosymmetric tetragonal structure (space group $P4\ mm$).¹⁾ Superconductivity with the transition temperature $T_{sc} = 0.75$ K is realized in the long-range antiferromagnetic ordered state with the Néel temperature $T_N = 2.2$ K. A large electronic specific heat coefficient $\gamma = 300 - 400$ mJ/K²·mol and a large slope of upper critical field dH_{c2}/dT ($= -8.5$ T/K) at T_{sc} suggest that superconductivity is based on heavy quasiparticles.

CePt₃Si is the first heavy-fermion superconductor lacking the inversion center in the crystal structure.^{1,2)} It has been thought that a material lacking inversion symmetry would be an unlikely candidate for spin-triplet pairing.^{3,4)} Interestingly, the upper critical field $H_{c2}(0)$ (~ 3 T) in CePt₃Si exceeds the Pauli-Clogston limit (~ 1 T), and triplet pairing was suggested in the superconducting state of CePt₃Si.¹⁾ Recent theoretical studies have claimed that the absence of the inversion center does not indiscriminately suppress the spin-triplet pairing state.⁵⁻¹⁰⁾ It should be noted that recently superconductivity was found in a ferromagnet UIr without inversion symmetry under pressure where the Curie temperature approximately becomes zero.¹¹⁾ The relation between anisotropic superconductivity and the non-centrosymmetric crystal structure is the most crucial issue to be clarified at present.

We grew a high-quality single crystal of CePt₃Si and investigated magnetic and electrical properties.^{12,13)} It was clarified that $H_{c2}(0)$ was approximately isotropic: $H_{c2}(0) = 2.7$ T for $H \parallel [100]$ and 3.2 T for $H \parallel [001]$. In the de Haas-van Alphen experiment, the topology of the Fermi surface in CePt₃Si was found to be most likely similar to that of LaPt₃Si. Large cyclotron masses of 10-20 m_0 were detected in CePt₃Si, which indicates

the existence of heavy quasiparticles in this compound. In the neutron scattering experiment, a clear antiferromagnetic Bragg peak with $Q = (0,0,1/2)$ was observed below T_N and the magnetic moment was determined as $0.16 \mu_B/\text{Ce}$.¹⁴⁾ The Bragg peak intensity was almost constant below T_{sc} , which indicates that the antiferromagnetic state coexists with the superconducting state. A microscopic coexistence between magnetism and superconductivity was also suggested by muon spin relaxation (μSR) and NMR experiments.¹⁵⁻¹⁷⁾ In particular, in the NMR experiment, the novel behavior of $1/T_1T$ ($1/T_1$: ¹⁹⁵Pt nuclear spin-lattice relaxation rate) was observed below T_{sc} , suggesting that a new class of superconducting state is realized in CePt₃Si.

Futhermore, the pressure dependence of the superconducting transition temperature T_{sc} was investigated by electrical resistivity measurements.^{18,19)} The transition temperature decreases with increasing pressure and finally becomes zero at 1.5 GPa. The Néel temperature T_N also decreases with increasing pressure, but the pressure dependence is not clear above 0.8 GPa because the change in the resistivity at T_N is too weak to be detected. In order to clarify the pressure phase diagram of CePt₃Si, we carried out heat capacity measurement under high pressures.

A detailed description of our sample preparation is given in the previous papers.^{12,13,18)} In the present heat capacity measurement, we used a high-quality single-crystal sample, which was cut from the sample used in the previous de Haas-van Alphen experiment. This sample was also used in the pressure experiment for the electrical resistivity and ac susceptibility. The sample size for the ac heat capacity measurement was $0.35 \times 0.25 \times 0.05$ mm³.

Heat capacity was measured by the ac calorimetry method in a piston cylinder pressure cell. The sample was thermally linked with a heat bath and was heated by application of an oscillating heating power $P =$

*This paper will be published in the July issue of J. Phys. Soc. Jpn.

†E-mail address: tateiwa@popsvr.tokai.jaeri.go.jp

$P_0[1+\cos(\omega t)]$, generated by a current of frequency $\omega/2$. The temperature oscillation T_{ac} at the same frequency ω was detected with a thermometer attached to the sample. Here, T_{ac} depends on the working frequency ω , the heat capacity of the sample C , and the thermal conductivity κ through the following equation^{20,21)} $T_{ac} = P_0/(\kappa + iC\omega)$, with $i^2 = -1$, under the assumption that the thermal relaxation in a sample is faster than $1/\omega$. When working above the cut-off frequency $\omega_1 = \kappa/C$, T_{ac} is inversely proportional to $C\omega$. The temperature oscillation T_{ac} was measured with a AuFe/Au thermocouple (Au + 0.07 at % Fe) with a diameter of 25 μm which was directly bonded to the sample. The thermovoltage V_{ac} is induced by the temperature difference between the sample at the temperature $(T_0 + \Delta T)$ and the edge of the sample chamber at T_0 . The value of T_{ac} is thus given as $T_{ac} = V_{ac}/S$, where S is the thermopower of a thermocouple. The sample was heated with a current supplied through Au wires with a diameter of 10 μm attached to the sample. Frequencies around 100 Hz were used for the measurement. In the present method, we could not determine the absolute value of the heat capacity. The Au-wires and thermocouple contribute to the heat capacity as a background. It is, however, noted that the signal is mainly due to the heat capacity of the sample at low temperatures because the volume ratio of the wires to the sample is in the order of a few %. The low-temperature measurement was performed using a ^3He - ^4He dilution refrigerator. We used a hybrid piston cylinder-type cell, where the Co-Ni-Cr-Mo (MP35N) inner cylinder was inserted into the Cu-Be outer sleeve.^{22,23)} As a pressure transmitting medium, Daphne oil (7373) was used.

Figure 1(a) shows the heat capacity C_{ac} under high pressures. Experimental data obtained under high pressures are shifted downwards. Here, C_{ac} corresponds to the inverse of the amplitude of the temperature oscillation T_{ac} . At ambient pressure, a clear heat capacity peak was observed at the Néel temperature T_N . The Néel temperature was determined as $T_N = 2.2$ K, as shown by an arrow. The heat capacity peak around T_N is of the λ -type, and the peak structure is sharper than those in the previous reports.^{1,12)} This might reflect the high quality of the present sample.

Below 0.5 K, the heat capacity indicates another peak due to the superconducting transition. The transition temperature T_{sc} is determined as $T_{sc} = 0.46$ K. The value is lower than those determined by the resistivity and ac magnetic susceptibility measurements (~ 0.7 K).¹²⁾ The reason for this discrepancy is not clear. Such a discrepancy was also found in the heavy fermion superconductor CeIrIn₅.²⁴⁾

The value of $\Delta C_{ac}/C_{ac}(T_{sc})$ is 0.33 at ambient pressure. Here, ΔC_{ac} is the jump of the heat capacity at T_{sc} and $C_{ac}(T_{sc})$ is the value of C_{ac} just above T_{sc} , namely, corresponding to γT_{sc} , where γ is the electronic specific heat coefficient. It is noted that a smaller value of 0.25 was reported in ref. 1. These values are far smaller than the BCS value $\Delta C/(\gamma T_{sc}) = 1.43$. This reduction might be due to the gapless structure of the anisotropic superconducting gap and/or the high sensitivity of the present superconductivity to impurities.

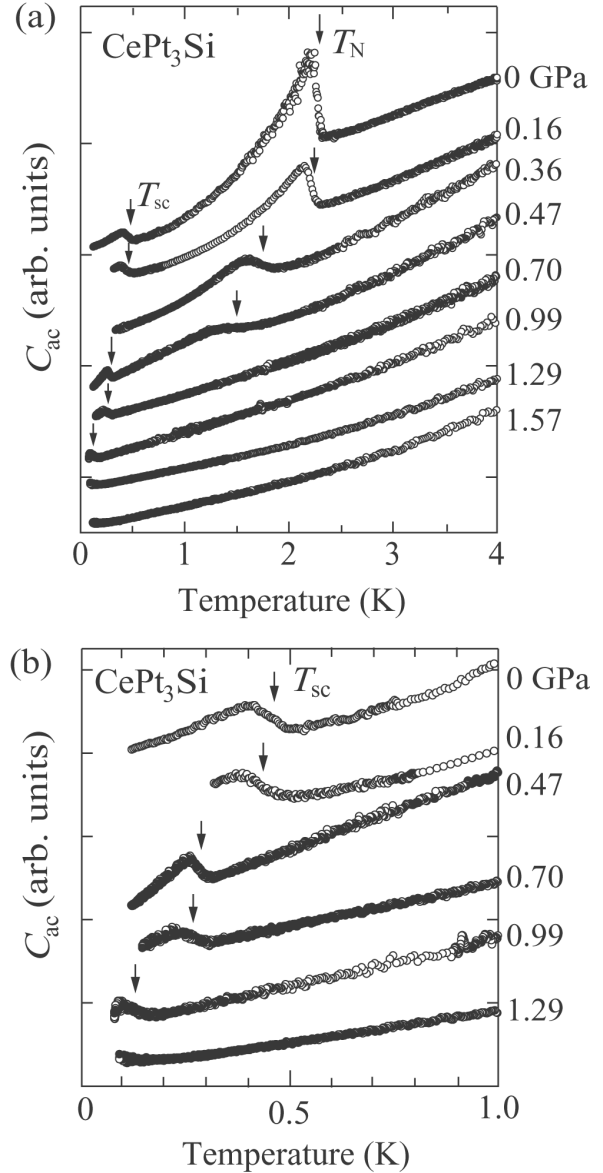


Fig. 1. (a) Temperature dependence of heat capacity C_{ac} and (b) low-temperature part of heat capacity C_{ac} of CePt₃Si under high pressures. Experimental data under high pressures are shifted downwards. T_N and T_{sc} correspond to the Néel temperature and superconducting transition temperature, respectively.

With increasing pressure, the antiferromagnetic ordering shifts to lower temperatures. The peak at $T_N = 2.2$ K becomes weak with increasing pressure and finally becomes a broad hump at 0.47 GPa. The peak was not observed in the C_{ac} curve at 0.70 GPa. This indicates that the antiferromagnetic ordering disappears at 0.70 GPa. The antiferromagnetic critical pressure P_{AF} was thus estimated as $P_{AF} \simeq 0.6$ GPa.

Figure 1(b) shows the low-temperature part of C_{ac} . The peak structure appears at T_{sc} under pressure. T_{sc} decreases with increasing pressure. The peak structure becomes weak at higher pressures. There is, however, no peak structure at 1.29 and 1.57 GPa (not shown in Fig. 1 (b)). The present result is approximately consistent with that of our previous resistivity measurement under high pressures; the superconducting critical pressure P_{sc} was

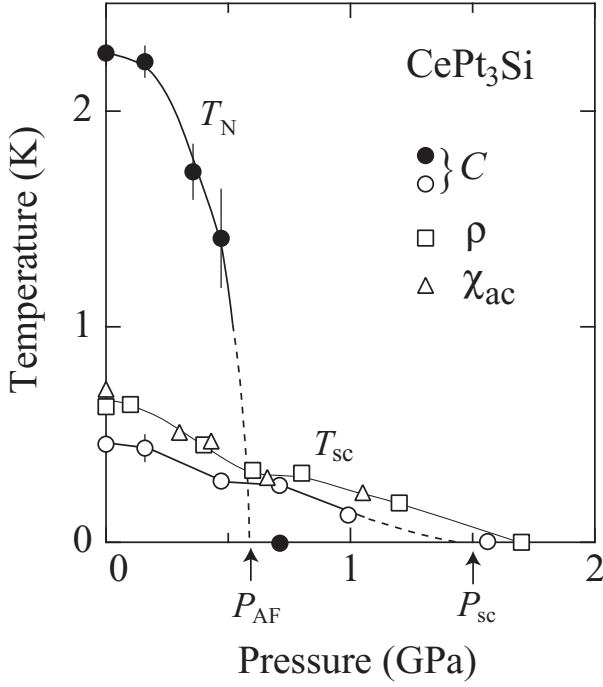


Fig. 2. Pressure phase diagram of CePt₃Si. The data shown by closed and open circles correspond to T_N and T_{sc} , respectively. The value of T_{sc} determined by the resistivity and ac susceptibility measurements are shown by open squares and triangles, respectively. Solid and dotted lines are guides to the eyes.

estimated as $P_{sc} \simeq 1.5$ GPa.¹⁸⁾ The T_{sc} value at 1.29 GPa might be below the lowest temperature of our measurement, 90 mK. In fact, C_{ac} shows an upturn structure below 130 mK at 1.29 GPa.

Figure 2 shows the pressure phase diagram of CePt₃Si determined by the present heat capacity measurement, together with the superconducting transition temperatures determined by our previous resistivity ρ and ac susceptibility χ_{ac} measurements.¹⁸⁾ We did not adopt the Néel temperature determined by the resistivity measurement in Fig. 2 because the change in the resistivity at T_N is very small. The T_N value decreases faster than that of T_{sc} with increasing pressure. An interesting point is that the superconducting phase exists above P_{AF} .

The pressure dependence of T_{sc} is characteristic, as shown in Fig. 2. Namely, T_{sc} decreases as a function of pressure, becomes approximately constant from 0.6 GPa to 0.8 GPa, decreases further with increasing pressure, and becomes zero at $P_{sc} \simeq 1.5$ GPa. The present pressure of 0.6 GPa corresponds to the antiferromagnetic critical pressure $P_{AF} \simeq 0.6$ GPa. In the pressure region from $P_{AF} \simeq 0.6$ GPa to 1.5 GPa, CePt₃Si is in the paramagnetic state and shows only the superconducting transition. The pressure phase diagram of CePt₃Si is thus very unique.

Figure 3(a) shows the pressure dependence of $\Delta C_{ac}/C_{ac}(T_{sc})$. It is almost constant in the pressure region from ambient pressure to P_{AF} and decreases steeply above $P_{AF} \simeq 0.6$ GPa. The value of $\Delta C_{ac}/C_{ac}(T_{sc})$ is, however, about 0.2 at 0.99 GPa. This indicates that the bulk superconducting state survives in the paramagnetic phase, namely above $P_{AF} \simeq 0.6$ GPa.

The thermocouple AuFe/Au is a dilute Kondo system

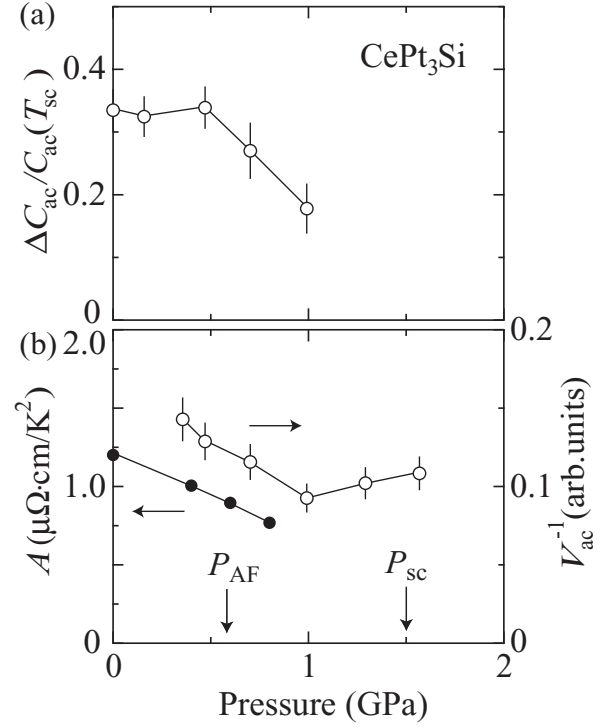


Fig. 3. (a) Pressure dependence of the jump of the heat capacity of CePt₃Si at T_{sc} . (b) Pressure dependences of the coefficient of the T^2 term in the resistivity (left side) and V_{ac}^{-1} (right side) for CePt₃Si.

and the thermopower $S(T)$ is given as $S(T) \propto T$ below 1 K. Therefore, the value of the inverse thermovoltage V_{ac}^{-1} , which corresponds to $[S(T)T_{ac}]^{-1}$, is approximately proportional to C/T at low temperatures. Therefore, the pressure dependence of V_{ac}^{-1} roughly corresponds to the electronic specific heat coefficient γ .

Figure 3(b) shows the pressure dependence of V_{ac}^{-1} , together with that of the coefficient A of the T^2 term in the electrical resistivity. Here, the data V_{ac}^{-1} was obtained just above T_{sc} under the same conditions of heater power P_0 , ac current frequency ω , and thermal conductivity κ . At 1.29 and 1.57 GPa, where the superconducting transition does not appear, V_{ac}^{-1} becomes almost constant below 0.2 K. This constant value is plotted in Fig. 3. The value of V_{ac}^{-1} decreases with increasing pressure and shows a tendency to saturate above 1.0 GPa, as shown in Fig. 3(b). Similarly, the A value simply decreases with increasing pressure and there is no anomaly around P_{AF} . These results indicate that there is no divergent feature in the pressure dependence of the electronic specific heat coefficient γ at P_{AF} and most likely at P_{sc} .

We will compare the present result for CePt₃Si with those for the other heavy-fermion Ce-based superconductors. In a prototype superconductor CeCu₂Si₂, superconductivity occurs in a nonmagnetic state that is close to antiferromagnetic instability.^{25,26)} The electronic state can be tuned by pressure or the stoichiometric composition of a sample. Superconductivity and antiferromagnetism are basically competitive and do not coexist in the compound. This is quite different from the characteristic feature of CePt₃Si. Namely, superconductivity coexists

with antiferromagnetism in CePt₃Si.

Another example is pressure-induced superconductivity in CeIn₃, CeRh₂Si₂, and CePd₂Si₂.^{27–31} These compounds show antiferromagnetic ordering at ambient pressure. T_N decreases with increasing pressure. Superconductivity appears around the magnetic critical region where T_N becomes zero, namely around P_{AF} . Superconductivity is considered to be mediated by low-energy magnetic excitations around the magnetic critical region where the heavy-fermion state is realized. The superconducting phase exists in a narrow pressure region around the magnetic critical region, and T_{sc} becomes a maximum around the critical pressure P_{AF} . These features are quite different from those of CePt₃Si where the bulk superconducting phase exists in a wide pressure region above and below P_{AF} , and T_{sc} does not show a maximum at P_{AF} . The maximum T_{sc} is realized at ambient pressure. The present superconductivity is most robust at ambient pressure. It is suggested from the pressure dependence of V_{ac} that the critical pressure P_{AF} is not of second order but of first one. Therefore, superconductivity in CePt₃Si is different from superconductivity associated with magnetic instability around the magnetic critical region.

The relation between antiferromagnetism and superconductivity in CePt₃Si is thus very unique. One might speculate that the superconducting and antiferromagnetic phases compete with each other below P_{AF} and the former overcomes the latter above P_{AF} . However, it should be noted that both ordering temperatures decrease with increasing pressure up to P_{AF} and that both T_{sc} and $\Delta C_{ac}/C_{ac}(T_{sc})$ decrease above P_{AF} . It seems to be difficult to consider these experimental results from a competitive relation between the two states. From the pressure dependence of T_{sc} , it is supposed that the coupling between the antiferromagnetic and superconducting states is basically weak. In order to clarify the relation between the two states, further study is needed. In particular, it is needed to investigate the change in the microscopic superconducting properties such as the paring symmetry across P_{AF} .

In conclusion, we constructed the pressure phase diagram of the heavy-fermion superconductor CePt₃Si by ac calorimetry. The bulk superconducting phase exists in a wide pressure region from ambient pressure to about 1.5 GPa, which is far above the antiferromagnetic critical pressure $P_{AF} \simeq 0.6$ GPa. The overall features of pressure phase diagram of CePt₃Si are different from those of the other heavy-fermion superconductors. Furthermore, it is emphasized, on the basis of the results of the present pressure experiment, that superconductivity in CePt₃Si is most robust at ambient pressure where the antiferromagnetic ordered state is realized.

Acknowledgments

One of authors (N.T) thanks Dr. M. -A. Méasson for helpful discussions. This work was financially supported by Grants-in-Aid for Young Scientists (B), Scientific Research (A), Creative Research (15GS0213), Scientific Research in Priority Area "Sukutterdite" (No. 16037215)

from the Ministry of Education, Culture, Sports, Science and Technology (Mext) and the Japanese Society for the Promotion of Science.

- 1) E. Bauer, G. Hilscher, H. Michor, Ch. Paul, E. W. Scheidt, A. Griбанov, Yu. Seropegin, H. Noël, M. Sigrist and P. Rogl: Phys. Rev. Lett. **92** (2004) 027003.
- 2) S. S. Saxena and P. Monthoux: Nature. **427** (2004) 799.
- 3) P. W. Anderson: Phys. Rev. B. **30** (1984) 4000.
- 4) M. Sigrist and K. Ueda, Rev. Mod. Phys. **63**, (1991) 239.
- 5) P. A. Frigeri, D. F. Agterberg, A. Koga and M. Sigrist: Phys. Rev. Lett. **92** (2004) 097001.
- 6) K. V. Samokhin, E. S. Zijlstra and S. K. Bose: Phys. Rev. B **69** (2004) 094514, Erratum: Phys. Rev. B **70** (2004) 069902(E).
- 7) I. A. Sergienko and S. H. Curnoe: Phys. Rev. B. **71** (2004) 214510.
- 8) K. V. Samokhin: Phys. Rev. Lett. **94** (2004) 027004.
- 9) P. A. Frigeri, D. F. Agterberg and M. Sigrist: New J. Phys. **6** (2004) 115.
- 10) V. P. Mineev: Phys. Rev. B. **71** (2005) 012509.
- 11) T. Akazawa, H. Hidaka, T. Fujiwara, T. C. Kobayashi, E. Yamamoto, Y. Haga, R. Settai and Y. Ōnuki: J. Phys.: Condens. Matter. **16** (2004) L29; J. Phys. Soc. Jpn. **73** (2004) 3129.
- 12) T. Takeuchi, S. Hashimoto, T. Yasuda, H. Shishido, T. Ueda, M. Yamada, Y. Obiraki, M. Shiimoto, H. Kohara, T. Yamamoto, K. Sugiyama, K. Kindo, T. D. Matsuda, Y. Haga, Y. Aoki, H. Sato, R. Settai and Y. Ōnuki: J. Phys.:Condens. Matter. **16** (2004) L333.
- 13) S. Hashimoto, T. Yasuda, T. Kubo, H. Shishido, T. Ueda, R. Settai, T. D. Matsuda, Y. Haga, H. Harima and Y. Ōnuki: J. Phys.:Condens. Matter. **16** (2004) L287.
- 14) N. Metoki, K. Kaneko, T. D. Matsuda, A. Galatanu, T. Takeuchi, S. Hashimoto, T. Ueda, T. D. Matsuda, Y. Ōnuki and N. Bernhoeft: J. Phys.:Condens. Matter. **16** (2004) L207.
- 15) A. Amato, E. Bauer and C. Baines: Phys. Rev. B. **71** (2005) 092501.
- 16) W. Higemoto, to be published.
- 17) M. Yogi, Y. Kitaoka, S. Hashimoto, T. Yasuda, R. Settai, Y. Ōnuki, P. Rogl and E. Bauer: Phys. Rev. Lett. **93** (2004) 027003.
- 18) T. Yasuda, H. Shishido, T. Ueda, S. Hashimoto, R. Settai, T. Takeuchi, T. D. Matsuda, Y. Haga and Y. Ōnuki : J. Phys. Soc. Jpn. **73** (2004) 1657.
- 19) M. Nicklas, G. Sparn, R. Lackner, E. Bauer and F. Steglich: Physica B **359-361** (2005) 386.
- 20) P. F. Sullivan and G. Seidel Phys. Rev. **173** (1968) 679.
- 21) H. Wilhelm: Adv. in Solid State Phys. **43** (2003) 889.
- 22) I. R. Walker: Rev. Sci. Instrum. **70** (1999) 3402.
- 23) Y. Uwatoko, S. Todo, K. Ueda, A. Uchida, M. Kosaka, N. Mori and T. Matsumoto: J. Phys.: Condens. Matter. **14** (2002) 11291.
- 24) C. Petrovic, R. Movshovich, M. Jaime, P. G. Paglusio, M. F. Hundley, J. L. Sarrao, Z. Fisk and J. D. Thompson; Europhys. Lett. **53** (2001) 354.
- 25) F. Steglich, J. Aarts, C-D Bredl, W. Lieke, D. Meschede, W. Franz and H. Schafer: Phys. Rev. Lett. **43** (1979) 1892.
- 26) H. Q. Yuan, F. M. Grosch, M. Deppe, C. Geibel, G. Sparn and F. Steglich: Science **302** (2003) 2104.
- 27) N D. Mathur, F M. Grosch, S. R. Julian, I. R. Walker, D. M. Freye, R. K. W. Haselwimmer and G. G. Lonzrich: Nature. **394** (1998) 39.
- 28) G. Knebel, D. Braithwaite, P. C. Canfield, G. Lapertot and J. Flouquet: Phys. Rev. B. **65** (2001) 024425.
- 29) R. Movshovich, T. Graf, D. Mandrus, J. D. Thompson, J. L. Smith and Z. Fisk: Phys. Rev. B. **53** (1996) 8241.
- 30) S. Araki, M. Nakashima, R. Settai, T. C. Kobayashi and Y. Ōnuki: J. Phys.: Condens. Matter. **14** (2002) L377.
- 31) A. Demuer, D. Jaccard, I. Sheikin, S. Raymond, B. Salce, J. Thomasson, D. Braithwaite and J. Flouquet: J. Phys.: Condens. Matter. **13** (2001) 9335.